N° d'enregistrement
au C.N.R.S. : AO 3452

ARTICLE PRINCIPAL

Recouvrant en partie

LA THESE DE DOCTORAT ES SCIENCES PHYSIQUES

présentée

A LA FACULTE DES SCIENCES

de PARIS

par

Monsieur Moiz RASIWALA

pour obtenir

le grade de Docteur ès Sciences

Sujet de la thèse : Dynamique des régions HII avec l'étoile excitatrice en mouvement

soutenue le 28 Juin 1969

devant la Commission d'Examen

MM.	Schatzman	Président
	Guiraud	Examinateurs
	Courtès	

N° d'enregistrement
au C.N.R.S. : AO 3452

ARTICLE PRINCIPAL

Recouvrant en partie

LA THESE DE DOCTORAT ES SCIENCES PHYSIQUES

présentée

A LA FACULTE DES SCIENCES

de PARIS

par

Monsieur Moiz RASIWALA

pour obtenir

le grade de Docteur ès Sciences

Sujet de la thèse : Dynamique des régions HII avec l'étoile excitatrice en mouvement

soutenue le 28 Juin 1969

devant la Commission d'Examen

MM.	Schatzman	Président
	Guiraud	Examinateurs
	Courtès	

Digitized by the Internet Archive
in 2026

UNIV.
LEIDEN
BIBL.

https://archive.org/details/IA41552220_0032

Astron. & Astrophys. 1, 431—441 (1969)

Dynamics of H II Regions with the Central Star in Motion

M. Rasiwala
Institut d'Astrophysique

Received November 29, 1968

The dynamics of an isothermal H II region is reconsidered for the case in which the central star is in motion. The deformation of the region is calculated (Figs. 2 to 5). It is found that the front changes from R- to D-type at different times depending on the polar angle and the stellar velocity (table). The flow is calculated along the axis of the H II region as defined by the rectilinear motion of the star. The equations are integrated numerically using a hodograph transformation and Riemann invariants. The results (Figs. 7 to 12) indicate a strong dissymmetry between the upstream and downstream regions.

Key words: interstellar gas, ionized — H II regions, aspherical due to stellar motion — H II regions, evolution with stellar motion

Introduction

In previous work on the dynamics of H II regions (Axford, 1961, 1964; Goldsworthy, 1961; Kahn, 1954; Kaplan, 1957; Lasker, 1966; Mathews, 1965; Savedoff and Greene, 1955; Vandervoort, 1963, 1964, 1966), the motion of the central exciting star has been neglected in order to arrive at the spherical symmetry necessary for a suitable simplification of the flow equations. However, since the central star is always in motion with respect to the surrounding medium, and often with a fairly high velocity, it is interesting to investigate how this motion will affect the over-all dynamics of H II regions. As a first step towards a solution of this problem, this paper attempts, under certain simplifying assumptions, to study two aspects of the question.

Firstly, we examine how an expanding H II region is deformed by the motion of the exciting star. A knowledge of the deformed surface is very important since it is the boundary conditions at this surface that will determine the nature of the flow.

Secondly, we try to obtain an estimate of the flow in the H II region. In this paper we use a one-dimensional model which should have some validity along the axis of the H II region, the axis being defined by the rectilinear motion of the star if rotational symmetry is assumed.

Before proceeding to an examination of the above questions, it is useful, however, to review very briefly the classification of ionization fronts. It may be asked whether the classification is still meaningful when the central star is in motion.

Classification of Ionization Fronts (Kahn, 1954)

Let the index 1 stand for the neutral region and the index 2 for the ionized region. Let $\boldsymbol{U}_1$ and $\boldsymbol{U}_2$ be the velocities of the gas at the front and with respect to it, and let $\boldsymbol{n}$ be the outward normal to the front. Then the following continuity conditions are satisfied at each instant if the front is considered to be a sharp discontinuity:

$$\begin{aligned} N_1(\boldsymbol{U}_1 \cdot \boldsymbol{n}) &= N_2(\boldsymbol{U}_2 \cdot \boldsymbol{n}) \\ N_1\{a_1^2 + (\boldsymbol{U}_1 \cdot \boldsymbol{n})^2\} &= N_2\{a_2^2 + (\boldsymbol{U}_2 \cdot \boldsymbol{n})^2\} \end{aligned} \tag{1}$$

where N = particle density and a = sound velocity.

By eliminating N_1 and N_2 from the above equations, it may easily be shown that $\boldsymbol{U}_2 \cdot \boldsymbol{n}$ has real values only if

$$|\boldsymbol{U}_1 \cdot \boldsymbol{n}| \geqq a_2 + (a_2^2 - a_1^2)^{1/2}$$

or if

$$|\boldsymbol{U}_1 \cdot \boldsymbol{n}| \leqq a_2 - (a_2^2 - a_1^2)^{1/2} .$$

The front is then of R-type or D-type respectively, and is R-critical or D-critical when the equality holds. A shock detaches itself from the front when the front becomes R-critical. Behind the shock the front is of D-type. The condition for the appearance of the shock is then

$$|\boldsymbol{U}_1 \cdot \boldsymbol{n}| = a_2 + (a_2^2 - a_1^2)^{1/2}$$

or

$$|\boldsymbol{U}_1 \cdot \boldsymbol{n}| \approx 2a_2 \tag{2}$$

if

$$a_2 \gg a_1 .$$

When the central star is not in motion, the condition (2) is uniformly satisfied at the front at a given moment of time. However, this is no longer the case when the exciting star is in motion as may be seen from the following consideration.

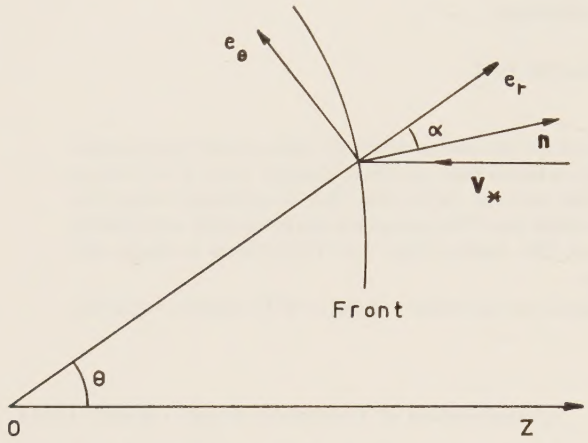

Fig. 1. The motion of the central star O is considered in a spherical coordinate system (r, θ, φ) in which O is at rest and there is a wind V_* as shown. $\boldsymbol{n}$, $\boldsymbol{e}_r$, $\boldsymbol{e}_\theta$ are unit vectors in the indicated directions, α is the angle between $\boldsymbol{n}$ and $\boldsymbol{e}_r$

Suppose the star to move along the positive z axis with a velocity $-\boldsymbol{V}_*$ (Fig. 1). We may consider the star to be at rest at the origin of a spherical system (r, θ, φ). The neutral medium will then stream past it with a velocity $\boldsymbol{V}_*$. Let $\boldsymbol{V}_F$ be the velocity of the ionization front. Then

$$\boldsymbol{U}_1 \cdot \boldsymbol{n} = (\boldsymbol{V}_* - \boldsymbol{V}_F) \cdot \boldsymbol{n} .$$

In particular, along the axis z, $\boldsymbol{n}$ is perpendicular to the front and $\boldsymbol{V}_F$ and $\boldsymbol{U}_1$ are along $\boldsymbol{n}$ and $-\boldsymbol{n}$ respectively, so that, if $X = |\boldsymbol{X}|$,

$$U_1(\theta = 0) = V_F + V_*$$

and (3)

$$U_1(\theta = \pi) = V_F - V_* .$$

From Eq. (2) a shock appears at $\theta = 0$ when $V_F = 2a_2 - V_*$ and at $\theta = \pi$ when $V_F = 2a_2 + V_*$. Since V_F is a function of time, it is obvious that a shock will detach itself from the front at different times depending on the polar angle. In particular, if $V_* > 2a_2$, it may be seen that U_1 will always be greater than $2a_2$ for a certain interval of the polar angle starting from 0, so that a shock cannot precede the front in this region. The table below shows the times $\mathscr{I}$ at which the shock separates from the front as a function of the polar angle and with the wind velocity V_* as parameter. The time at which the shock separates from a spherical front is taken as unit time. This table is obtained from an equation to be derived later.

Table. *The times $\mathscr{I}$ at which the shock separates from an R-type H II region at different polar angles and for different wind velocities*

Unit time is the one for which a shock separates from a spherical H II region (zero wind velocity).

V_* km/s / θ	0°	30°	60°	90°	120°	150°	180°
10	1.48	1.39	1.21	1.02	0.88	0.80	0.78
20	∞	3.22	1.73	1.10	0.81	0.68	0.64
100	—	—	—	—	0.92 (127°)	0.35	0.29

It is obvious from the above table that the front can only locally be of R- or D-type.

Deformation of the H II Region

Gould (1963) has already calculated the shape of an H II region in which the central star is in motion. However, he neglects the hydrodynamic flow field in this region, assuming a uniform, steady streaming of the medium past the star. We assume no knowledge of the flow field behind the ionization front in order to calculate the surface, since the flow will be determined by the surface.

Although Vandervoort (1966) has shown that the rate of contraction of the star onto the main sequence is essential in determining even the qualitative nature of the flow, we will assume the star to be a point source of radiation which is "switched on" instantaneously at a time $t = 0$ and radiates thereafter at constant main-sequence intensity. Under these circumstances, it is well known that the ionization front will move supersonically into the neutral gas ahead so that the latter will be incident blindly on the front. We will consider only these early supersonic stages of the front. The velocity field in the H I region is then simply given by $\boldsymbol{V}_*$ at each instant. In addition, we will assume that the absorption of the ionizing radiation within the H II region is negligible so that all of the stellar radiation reaches the front. Let $r_F = r_F(\theta, t)$ be the radius of the H II region. (The problem being axially symmetric, there is no dependence on φ.) Let $\boldsymbol{e}_r$ and $\boldsymbol{e}_\theta$ be unit vectors along $\boldsymbol{r}$ and $\boldsymbol{\theta}$ respectively and let α

be the angle between $\boldsymbol{n}$ and $\boldsymbol{e}_r$ (Fig. 1). If the star emits S ionizing photons per unit time, then the flux at the front, and normal to it, is given by $S \cos \alpha / 4 \pi r_F^2$. Finally, we will suppose that the mass density ϱ_1 is constant in the H I region and that the front is a sharp discontinuity with complete ionization on the one side and zero ionization on the other. Each neutral atom is then immediately ionized upon crossing the front and the following equality holds at each instant:

Flux of neutral atoms crossing the front normally = Flux of ionizing photons arriving normally at the front. (4)

Since the velocity of the front

$$\boldsymbol{V}_F = \frac{d r_F}{d t} \boldsymbol{e}_r + r_F \frac{d \theta}{d t} \boldsymbol{e}_\theta$$

and the normal $\boldsymbol{n} = \boldsymbol{e}_r \cos \alpha - \boldsymbol{e}_\theta \sin \alpha$, the condition (4) immediately yields

$$\varrho_1 (\boldsymbol{V}_* - \boldsymbol{V}_F) \cdot \boldsymbol{n} = \frac{-m_H S}{4 \pi r_F^2} \frac{1}{\sqrt{1 + \left(\frac{1}{r_F} \frac{\partial r_F}{\partial \theta}\right)^2}} \tag{5}$$

where m_H = mass of the hydrogen atom and $\frac{1}{r_F} \frac{\partial r_F}{\partial \theta} = \tan \alpha$ (Fig. 1). The minus sign accounts for the fact that the two fluxes are oppositely directed. Substituting for $\boldsymbol{n}$, and using the condition

$$d r_F = \frac{\partial r_F}{\partial t} d t + \frac{\partial r_F}{\partial \theta} d \theta ,$$

we obtain, after simplification,

$$\frac{\partial r_F}{\partial t} + \frac{V_*}{r_F} \frac{\partial r_F}{\partial \theta} \sin \theta = \frac{C - V_* r_F^2 \cos \theta}{r_F^2} \tag{6}$$

where

$$C = \frac{m_H S}{4 \pi \varrho_1} = \frac{S}{4 \pi N_1} ,$$

N_1 being the particle density in the H I region. Further, we have put $\boldsymbol{V}_* \cdot \boldsymbol{e}_r = - V_* \cos \theta$, and $\boldsymbol{V}_* \cdot \boldsymbol{e}_\theta = V_* \sin \theta$.

The solution of this quasi-linear equation will give us the desired form of the surface. It is convenient to rewrite it in terms of non-dimensional varibles as follows.

We define a distance r_0 such that, at this distance, a shock just detaches itself from a spherical front (one for which the central star is at rest), i.e., the velocity V_{Fs} of the spherical front becomes equal to $2 a_2$, according to Eq. (2). From condition (4):

$$\frac{d r_{Fs}}{d t} = V_{Fs} = \frac{S}{4 \pi N_1 r_{Fs}^2} = \frac{C}{r_{Fs}^2} , \tag{7}$$

so that

$$r_0^2 = \frac{C}{2 a_2} , \tag{8}$$

Further, let t_0 be the time at which the spherical front has a radius r_0. From (7), $r_{Fs}^3 = 3 C t$, so that,

$$t_0 = \frac{r_0^3}{3 C} = \frac{r_0}{6 a_2} . \tag{9}$$

Introducing the non-dimensional variables

$$\mathscr{I} = \frac{t}{t_0} \quad \text{and} \quad \mathscr{R} = \frac{r_F}{r_0} \tag{10}$$

we can rewrite Eq. (5) as follows,

$$\frac{\partial \mathscr{R}}{\partial \mathscr{I}} + \frac{\mathscr{V}_* \sin \theta}{6 \mathscr{R}} \frac{\partial \mathscr{R}}{\partial \theta} = \frac{2 - \mathscr{V}_* \mathscr{R}^2 \cos \theta}{6 \mathscr{R}^2} \tag{11}$$

where

$$\mathscr{V}_* = \frac{V_*}{a_2} .$$

We look for a solution of Eq. (11) which satisfies the initial condition $\mathscr{R} = 0$ for $\mathscr{I} = 0$ and any θ, i.e., a solution which in $\mathscr{R} \mathscr{I} \theta$ space passes through the θ-axis.

Equation (11) is easily solved by the method of characteristics (Courant and Hilbert, 1962, Ch. II). The characteristic curves through a point $\mathscr{R} \mathscr{I} \theta$ are given by the relations

$$d \mathscr{I} = \frac{6 \mathscr{R} d \theta}{\mathscr{V}_* \sin \theta} = \frac{6 \mathscr{R}^2 d \mathscr{R}}{2 - \mathscr{V}_* \mathscr{R}^2 \cos \theta} . \tag{12}$$

Every surface generated by the above characteristic curves is an integral surface of Eq. (11). In particular, we look for an integral surface which passes through the initial curve

$$\mathscr{R} = 0 , \quad \mathscr{I} = 0 , \quad \theta = \theta_s , \quad 0 \leqq \theta_s \leqq \pi . \tag{13}$$

Let s be a parameter along the initial curve. Then the initial value problem has a unique solution if

$$\Delta = \frac{\partial \theta}{\partial s} - \frac{\mathscr{V}_* \sin \theta}{6 \mathscr{R}} \frac{\partial \mathscr{I}}{\partial s} \neq 0$$

along the initial curve (Courant and Hilbert, 1962, Ch. II). From Eqs. (12) and (13) it is easily verified that the above condition is satisfied, so that the imitial value problem has a unique solution.

From (12) and (13), we get:

$$\mathscr{R}^2 = \frac{4}{\mathscr{V}_*} \frac{\cos \theta_s - \cos \theta}{\sin^2 \theta} . \tag{14}$$

From (12) and (14), we obtain:

$$\mathscr{I} = \int_0^{\mathscr{R}} \frac{6 \mathscr{R}^2 d \mathscr{R}}{\sqrt{\mathscr{R}^4 \mathscr{V}_*^2 - 4 \mathscr{V}_* \cos \theta_s \mathscr{R}^2 + 4}} + K , \tag{15}$$

where K is an arbitrary constant. The polynomial in $\mathscr{R}$ under the square root sign can be written in the form

$$\mathscr{V}_*^2 \left[\left\{\mathscr{R} + \sqrt{\frac{1+\cos\theta_s}{\mathscr{V}_*}}\right\}^2 + \left(\frac{1-\cos\theta_s}{\mathscr{V}_*}\right)\right] \cdot \left[\left\{\mathscr{R} - \sqrt{\frac{1+\cos\theta_s}{\mathscr{V}_*}}\right\}^2 + \left(\frac{1-\cos\theta_s}{\mathscr{V}_*}\right)\right]$$

If $\cos\theta_s \neq 1$, then the elliptic integral in Eq. (15) can be expressed in terms of normal elliptic integrals (Gröbner and Hofreiter, 1949, p. 91, 8 C 8). Applying the initial conditions (13), introducing the values of $\cos\theta_s$ from Eq. (14) and using the addition formulae for elliptic integrals (Byrd and Friedman, 1954, see 116.01), we obtain, after a considerable amount of simplification,

$$\mathscr{I} = \frac{6}{\mathscr{V}_*^{3/2}} \left[A\, F(\varphi, k) - B\, E(\varphi, k) + D\right], \quad (16)$$

where

$$F(\varphi, k) = \int_0^{\varphi} \frac{d\varphi'}{\sqrt{1 - k^2 \sin^2\varphi'}}$$

and

$$E(\varphi, k) = \int_0^{\varphi} \sqrt{1 - k^2 \sin^2\varphi'}\; d\varphi'$$

are the normal elliptic integrals of the first and second kind respectively. Further,

$$A = \frac{P^2}{2\{2\sqrt{2} + P\}};$$

$$B = \frac{2\sqrt{2} + P}{2};$$

$$D = P \sin\varphi \left(\sqrt{2} + \mathscr{R}\sqrt{\mathscr{V}_*}\right) - \frac{P}{2} + \frac{P + 2\mathscr{R}\sqrt{\mathscr{V}_*}}{2} \times \left(\frac{\mathscr{R}^2 \mathscr{V}_* - P\mathscr{R}\sqrt{\mathscr{V}_*} + 2}{\mathscr{R}^2 \mathscr{V}_* + P\mathscr{R}\sqrt{\mathscr{V}_*} + 2}\right)^{1/2},$$

$$\varphi = 2 \arctan \left[\frac{(\sqrt{2} + \mathscr{R}\sqrt{\mathscr{V}_*}) - (\mathscr{R}^2 \mathscr{V}_* - P\mathscr{R}\sqrt{\mathscr{V}_*} + 2)^{1/2}}{(\sqrt{2} - \mathscr{R}\sqrt{\mathscr{V}_*}) + (\mathscr{R}^2 \mathscr{V}_* + P\mathscr{R}\sqrt{\mathscr{V}_*} + 2)^{1/2}}\right]$$

and

$$k^2 = \frac{8\sqrt{2}\,P}{(2\sqrt{2} + P)^2}$$

with

$$P = (4 + \mathscr{R}^2 \mathscr{V}_* \sin^2\theta + 4\cos\theta)^{1/2} \quad (17)$$

Equation (16) is the desired solution of Eq. (11). It is not possible, from Eq. (16), to obtain an expression for $\mathscr{R}$ as a function of $\mathscr{I}$ and θ. Hence the shape of the front at different times was obtained numerically using a subroutine for implicit equations. The sound speed a_2 was taken to be 10 km/s, the H II region being considered isothermal at 10000°.

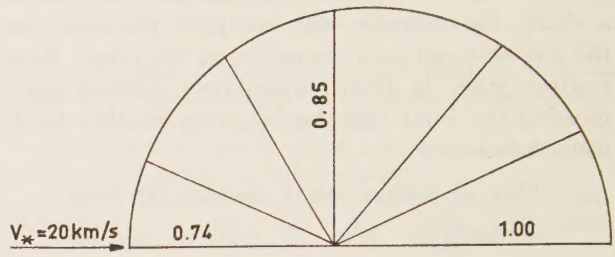

Fig. 2. The deformation of the H II region at $\mathscr{I} = 0.64$ for a wind velocity of 20 km/s. The radii $\mathscr{R}$ are measured in terms of the radius of a spherical R-critical front, this radius being taken as unity. A shock separates from the spherical front when $\mathscr{I} = \mathscr{R} = 1$

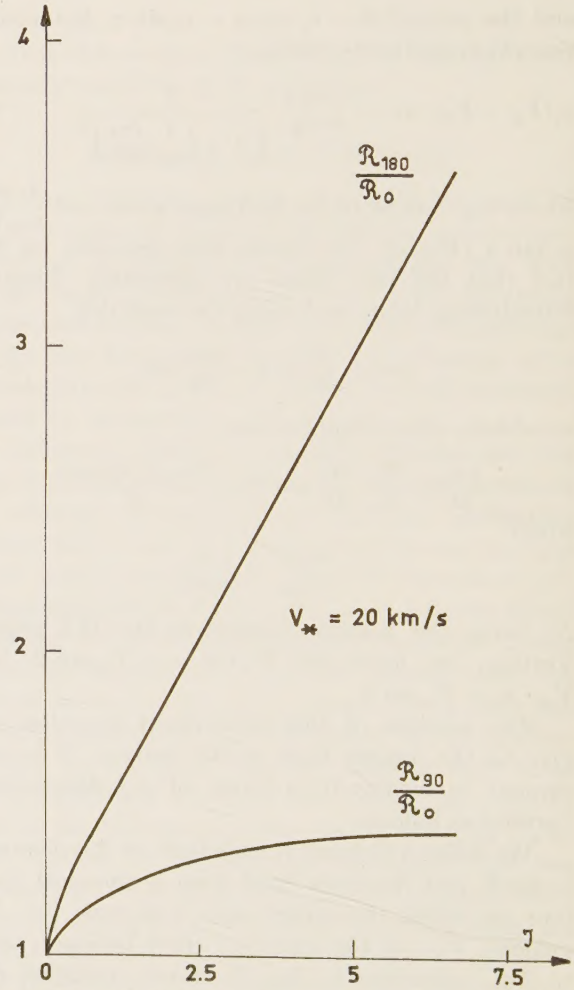

Fig. 3. The ratios of the non-dimensional radii of the H II region at $\theta = 0°$, 90° and 180° are plotted as a function of the non-dimensional time $\mathscr{I}$ for a wind velocity of 20 km/s

Fig. 2 shows the shape of the front at $\mathscr{I} = 0.64$ when the shock just separates from the front at $\theta = \pi$. If $\mathscr{R}_n$ be the radius at $n°$, it is seen that, at $\mathscr{I} = 0.64$, $\mathscr{R}_{\pi/2}/\mathscr{R}_0 = 1.15$ and $\mathscr{R}_\pi/\mathscr{R}_0 = 1.35$. Figs. 3 and 4 show these two ratios as a function of time for the wind velocities 20 km/s and 100 km/s respectively. As to be expected, the deformation is very slight at the beginning but becomes more and more pronounced as the front slows down. Also, at a given time, the deformation increases rapidly with wind velocity. For e.g., at $\mathscr{I} = 0.29$ already and $V_* = 100$ km/s (shock just separating at $\theta = \pi$), $\mathscr{R}_{\pi/2}|\mathscr{R}_0 = 1.34$ whereas $\mathscr{R}_\pi|\mathscr{R}_0 = 2.28$.

Equation (16) yields a limiting form for the H II region. In fact, as $P \to 2\sqrt{2}$ in Eqs. (17), $k^2 \to 1$ and $\varphi \to \pi/2$. Since $F(\pi/2, 1) = \infty$ (Byrd et al., 1954, see 111.05), we see that $\mathscr{I} \to \infty$ as $P \to 2\sqrt{2}$, i.e. as $(4 + \mathscr{R}^2 \mathscr{V}_* \sin^2\theta + 4\cos\theta)^{1/2} \to 2\sqrt{2}$. Thus the limiting value of in $\mathscr{R}$ any direction θ is given by

$$\mathscr{R}^2_{\max} = \frac{4}{\mathscr{V}_*(1 + \cos\theta)} \,. \tag{18}$$

We note that the limiting value corresponds to $\cos\theta_s = 1$ in Eq. (14), and that the ratio

$$\mathscr{R}_{\max}(\theta_1)/\mathscr{R}_{\max}(\theta_2)$$

for any two θ_1 and θ_2 is independent of $\mathscr{V}_*$.

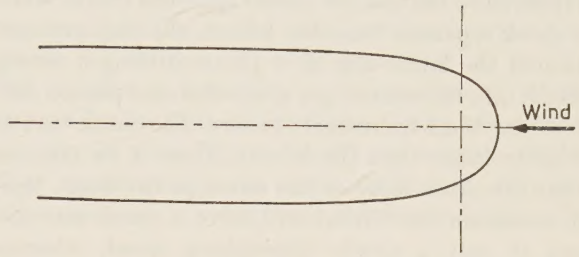

Fig. 5. The limiting form of an H II region in presence of a wind caused by stellar motion. The shape of the limiting surface is independent of the wind velocity V_*, the scale diminishing as $1/V_*^{1/2}$

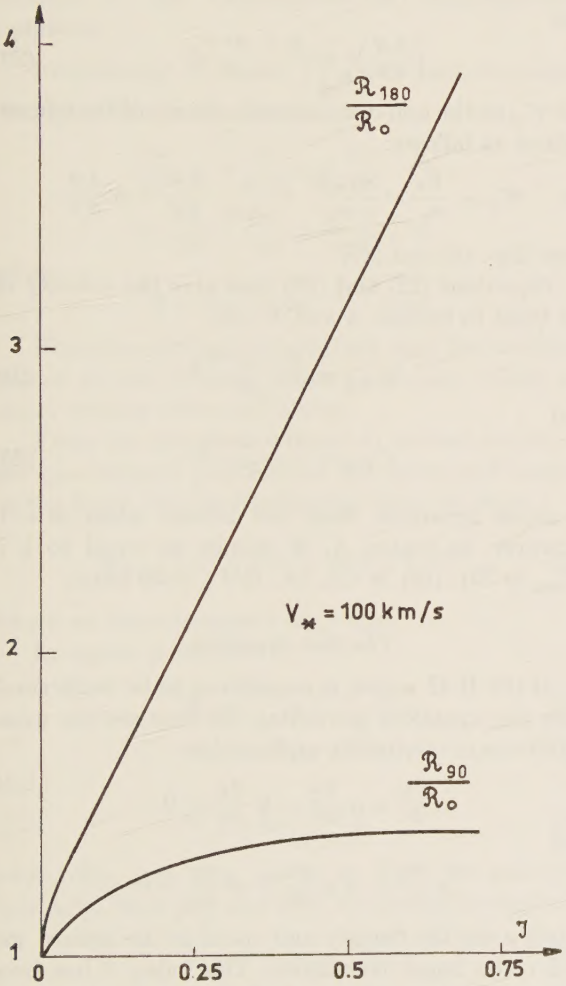

Fig. 4. Same as Fig. 3 with $V_* = 100$ km/s

The limiting form of the H II region is shown in Fig. 5. Its physical meaning is obvious. In front of the star, expansion stops when the expansion velocity becomes equal to the opposing wind velocity in that direction, whereas behind the star, the wind ultimately aligns the H II region in its own direction. However, there is never a steady state since the establishment of such a region takes infinite time. Also, the region extends to infinity at the back of the star since we have neglected the absorption of the ionizing photons.

Finally, the shock appears at any given angle when $|\boldsymbol{U}_1 \cdot \boldsymbol{n}| = 2\,a_2$. Writing $\boldsymbol{U}_1 = \boldsymbol{V}_* - \boldsymbol{V}_F$ and proceeding as in Eqs. (5) to (11), it may be shown that the condition for the appearance of a shock in any given direction is given by

$$\mathscr{R}^2 \sqrt{1 + \left(\frac{1}{\mathscr{R}} \frac{\partial \mathscr{R}}{\partial \theta}\right)^2} = 1 \,, \tag{19}$$

where $\partial\mathscr{R}/\partial\theta$ is to be evaluated at a given $\mathscr{I}$ and θ from Eq. (16). Equations (16) and (19) were solved simultaneously in order to obtain the values given in the table. It may be noted that, at $\theta = 0$ and π, $\partial\mathscr{R}/\partial\theta = 0$ for all $\mathscr{I}$, so that the shock appears when $\mathscr{R} = 1$.

Conclusion

If we consider the peculiar velocity of a hot star to be typically 20 km/s and time-scales about equal to the time when the shock separates at 180°, then little deformation might be expected in these early stages of the front. In later stages, a shock precedes at least a certain portion of the front downstream, and evolves with time, so that we have to take into account a complicated non-steady flow field in the compressed region.

However, the detailed calculations of Lasker (1966) show that, in the case of spherical fronts, when a shock separates from the I-front, the high pressure behind the latter acts as a piston driving a strong shock into the neutral gas even when the photon flux reaching the I-front tends to zero. The shock travels slightly faster than the I-front. Thus, if we imagine that the shock more or less envelops the front, then downstream the I-front will drive a shock into the gas at only a slowly diminishing speed, whereas upstream there will be either no shock at all, or both the shock and the I-front will move only very slowly. Under these circumstances the deformation will increase rapidly with time even in presence of a shock.

For an O 7 star with an ionizing photon luminosity of $2.45 \times 10^{48}\ \mathrm{s}^{-1}$, a shock separates from the gas at a time equal to 1.3×10^5 years (Lasker, 1966) if $N_1 = 6.4\ \mathrm{cm}^{-3}$. As we have shown, the shock separates much earlier from the front downstream when the central star is in motion, so that we might expect significant deformation in H II regions about 10^5 years old. The author hopes to consider the morphological aspects of H II regions with shocks in a future publication.

Finally, we note that for wind velocities of the order of 100 km/s, a considerable deformation will be produced already at times of the order of $\mathscr{I} = 0.3$, i.e. 4×10^4 years if t_0 in Eq. (10) is taken to be of the order of 1.3×10^5 years.

Flow Along the Axis of the H II Region

In this paper we consider the flow only along the axis of the H II region as defined by $\theta = 0$ and $\theta = \pi$ in Fig. 1. It is hoped that this will give us at least an idea of the kind of modifications which the motion of the central star introduces in the dynamics of H II regions.

In the framework indicated in Fig. 1, we will call region A, the region extending upstream from the star O, and region B, the region extending downstream. The integral (15) was reduced to normal elliptic integrals under the assumption that $\cos\theta_s \neq 1$. From Eq. (14) we see that $\cos\theta_s = 1$ when $\theta = 0$. Thus Eq. (16) is not valid for $\theta = 0$. However, by putting $\theta = 0$ in Eq. (11) we obtain an expression for $\mathscr{I}_A$, viz,

$$\mathscr{I}_A = \frac{6}{\mathscr{V}_*}\left\{\frac{1}{\sqrt{2\,\mathscr{V}_*}}\ln\frac{\sqrt{2}+\mathscr{R}\sqrt{\mathscr{V}_*}}{\sqrt{2}-\mathscr{R}\sqrt{\mathscr{V}_*}} - R\right\} \tag{20}$$

which gives the position of the front in region A. For the region B, we may put $\theta = \pi$ in Eqs. (16) and (17). Remembering that $F(\varphi, 0) = E(\varphi, 0) = \varphi$ (Byrd, Friedman, 1954, see 111.01), we obtain,

$$\mathscr{I}_B = \frac{6}{\mathscr{V}_*}\left\{\mathscr{R} - \sqrt{\frac{2}{\mathscr{V}_*}}\ \mathrm{arc\,tan}\ \mathscr{R}\sqrt{\frac{\mathscr{V}_*}{2}}\right\}. \tag{21}$$

Further, by differentiating Eqs. (20) and (21) with respect to $\mathscr{I}$ we obtain

$$\left(\frac{\partial\mathscr{R}}{\partial\mathscr{I}}\right)_A = \frac{2-\mathscr{R}^2\mathscr{V}_*}{6\,\mathscr{R}^2} \tag{22}$$

and

$$\left(\frac{\partial\mathscr{R}}{\partial\mathscr{I}}\right)_B = \frac{2+\mathscr{R}^2\mathscr{V}_*}{6\,\mathscr{R}^2}. \tag{23}$$

Let $\mathscr{V}_F$ be the non-dimensional velocity of the I-front, defined as follows:

$$\mathscr{V}_F = \frac{V_F}{a_2} = \frac{dr_F/dt}{a_2} = \frac{r_0}{t_0\,a_2}\frac{d\mathscr{R}}{d\mathscr{I}} = 6\frac{d\mathscr{R}}{d\mathscr{I}}$$

from Eqs. (9) and (10).

Equations (22) and (23) then give the velocity of the front in regions A and B, viz,

$$\mathscr{V}_{FA} = \frac{2-\mathscr{R}^2 V_*}{\mathscr{R}^2} \tag{24}$$

and

$$\mathscr{V}_{FB} = \frac{2+\mathscr{R}^2 V_*}{\mathscr{R}^2}. \tag{25}$$

A shock separates from the I-front when $\mathscr{R} = 1$. However, in region A, $\mathscr{R}$ cannot be equal to 1 if $\mathscr{R}_{\max}$ in Eq. (18) is <1, i.e., if $V_* > 20$ km/s.

The flow equations

If the H II region is considered to be isothermal, then the equations governing the flow are the usual equations of continuity and motion:

$$\frac{\partial\varrho}{\partial t} + \varrho\frac{\partial u}{\partial r} + u\frac{\partial\varrho}{\partial r} = 0$$

and

$$\varrho\frac{\partial u}{\partial t} + \varrho\,u\frac{\partial u}{\partial r} + a^2\frac{\partial\varrho}{\partial r} = 0.$$

ϱ and u are the density and speed in the ionized gas and r the linear coordinate. The index 2 has been dropped for convenience.

The continuity equation written in the above form is correct only if the motion is strictly one-dimensional with the velocities everywhere parallel to the axis. In the actual H II region even the material on the axis will be affected by transverse motions so that $\operatorname{div} \boldsymbol{u} \neq \partial u/\partial r$. However, in this article we are considering only the early, supersonic stages of an I-front. It is well known that in these early stages the front corresponds to a weak shock, neither the gas density nor its velocity state being much affected by the passage of the front. Now the deflection of a streamline by a weak shock is insignificant even if the shock is quite oblique (Landau and Lifschitz, 1959, p. 335). But we are considering only the axis of the H II region. The shock is not only weak but almost a normal shock. Thus, to a reasonable degree of approximation, we may treat the velocity field near the axis as a parallel flow and use $\operatorname{div} \boldsymbol{u} \equiv \partial u/\partial r$. Later stages of the front require a solution of the two-dimensional time-dependent equations.

Introducing $\mathscr{U} = a \ln\left(\frac{\varrho}{\varrho_1}\right)$ and non-dimensionalising as before, we obtain,

$$\begin{aligned} \frac{\partial \mathscr{U}}{\partial \mathscr{R}} + \mathscr{U}\frac{\partial \mathscr{V}}{\partial \mathscr{R}} + 6\frac{\partial \mathscr{V}}{\partial \mathscr{I}} &= 0\,, \\ \mathscr{U}\frac{\partial \mathscr{U}}{\partial \mathscr{R}} + \frac{\partial \mathscr{V}}{\partial \mathscr{R}} + 6\frac{\partial \mathscr{U}}{\partial \mathscr{I}} &= 0\,, \end{aligned} \tag{26}$$

where

$$\mathscr{U} = u/a \quad \text{and} \quad \mathscr{V} = v/a\,.$$

Equations (26) are to be solved with the boundary values at the I-front. These boundary values are easily written down as follows.

From the jump conditions (1) we can obtain u_2, the gas velocity just behind the front with respect to the front. In non-dimensional form we have

$$\mathscr{U}_2 = \frac{u_2}{a_2} = \frac{1}{2}\{\mathscr{U}_1 + (\mathscr{U}_1^2 - 4)^{1/2}\}\,, \tag{27}$$

where we have supposed $\mathscr{U}_1 \gg a_1/a_2$.

In region A we have

$$\mathscr{U}_{1A} = \mathscr{V}_* + \mathscr{V}_{FA}\,, \tag{28}$$

$$\mathscr{U}_A = \mathscr{U}_{2A} - \mathscr{V}_{FA}\,, \tag{29}$$

and

$$\mathscr{V}_A = \ln\left(\frac{\mathscr{U}_{1A}}{\mathscr{U}_{2A}}\right), \tag{30}$$

where $\mathscr{U}_{2A}$ and $\mathscr{V}_{FA}$ are as in Eqs. (24) and (27). Similarly, from (25) and (27), we obtain for region B,

$$\mathscr{U}_{1B} = \mathscr{V}_{FB} - \mathscr{U}_{2B}\,, \tag{31}$$

$$\mathscr{U}_B = \mathscr{V}_{FB} - \mathscr{U}_{2B}\,, \tag{32}$$

and

$$\mathscr{V}_B = \ln\left(\frac{\mathscr{U}_{1B}}{\mathscr{U}_{2B}}\right). \tag{33}$$

(29), (30), (32) and (33) are the boundary values for $\mathscr{U}$ and $\mathscr{V}$ in the regions A and B respectively.

The Boundary Value Problem

It is easy to show that the boundary values of $\mathscr{U}$ and $\mathscr{V}$ determine a unique solution of the flow Eqs. (26) in the ionized region.

For the spherical case, Vandervoort (1963a, b) has considered the initial value problem in which the values for $\mathscr{U}$ and $\mathscr{V}$ were prescribed at $\mathscr{I} = 0$. We consider a boundary value problem in which boundary conditions are prescribed along two arcs in the $\mathscr{R} - \mathscr{I}$ plane, and we look for a solution of the flow equations in the region contained between these two arcs (Courant and Friedrichs, 1948).

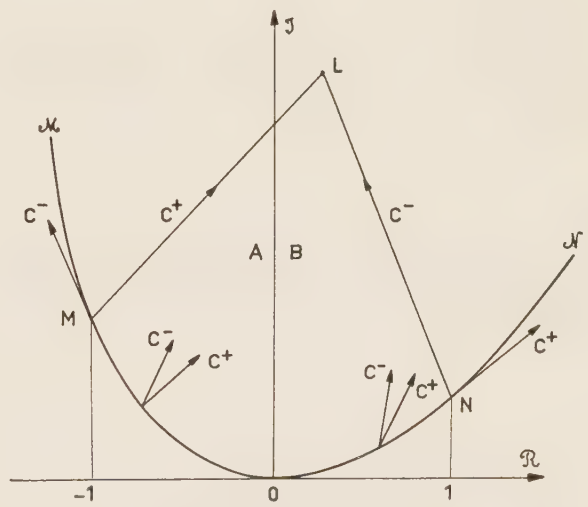

Fig. 6. The characteristic diagram in the $\mathscr{R} - \mathscr{I}$ plane. $\mathscr{M}$ and $\mathscr{N}$ are the paths of the I-front upstream and downstream respectively. C^+ and C^- are characteristics. $\mathscr{M}$ and $\mathscr{N}$ are space-like up to M and N, time-like thereafter. A unique solution for the flow exists in the ionized region LMON

The paths of the I-front in the $\mathscr{R} - \mathscr{I}$ plane are given by Eqs. (20) and (21). Typical paths $\mathscr{M}$ and $\mathscr{N}$ are shown in Fig. 6. Let M and N be points on $\mathscr{M}$ and $\mathscr{N}$ such that $\mathscr{R} = \pm 1$ at these points. Since the flow problem is hyperbolic, there are two different characteristic directions through each point on $\mathscr{M}$ and $\mathscr{N}$. These characteristic directions C^+ and C^- are given by $dr/dt = u \pm a$, or, in non-dimensional

variables,

$$\frac{\partial \mathscr{R}}{\partial \mathscr{I}} = \frac{1}{6}(\mathscr{U} \pm 1) . \tag{34}$$

It can be verified from Eqs. (22), (23) and (27) to (33) that as long as $-1 < \mathscr{R} < 1$, both characteristic directions lie to the right of $\mathscr{M}$ in region A and to the left of $\mathscr{N}$ in region B. At $\mathscr{R} = \pm 1$, $\mathscr{M}$ becomes characteristic in the direction of C^- and $\mathscr{N}$ in the directions of C^+ (Fig. 6). Thus $\mathscr{M}$ and $\mathscr{N}$ are both space-like up to $\mathscr{R} = \pm 1$ and time-like thereafter (Courant and Friedrichs, 1948).

Let the C^+ direction at M interest the C^- direction at N in the point L. Then all points within the region LMON have their domains of dependence on MON. Further, we know that a unique solution exists in the region LMON and that the space-like two-data given by Eqs. (29), (30), (32) and (33) are sufficient to determine the unique solution (Courant and Friedrichs, 1948).

The Resolution of the Flow Equations

The most convenient way to solve Eqs. (26) is to interchange the roles of the dependent and independent variables (hodograph transformation). This is always possible if the determinant

$$\frac{\partial(\mathscr{R}, \mathscr{I})}{\partial(\mathscr{U}, \mathscr{V})} \neq 0 ,$$

i.e. if a finite area in the $\mathscr{R} - \mathscr{I}$ plane is mapped into a finite area in the $\mathscr{U} - \mathscr{V}$ plane. Using $\mathscr{U}$ and $\mathscr{V}$ as the new independent variables, Eqs. (26) can be written

$$\begin{aligned} &\frac{\partial \mathscr{I}}{\partial \mathscr{V}} - \mathscr{U}\frac{\partial \mathscr{I}}{\partial \mathscr{U}} + 6\frac{\partial \mathscr{R}}{\partial \mathscr{U}} = 0 , \\ &\mathscr{U}\frac{\partial \mathscr{I}}{\partial \mathscr{V}} - \frac{\partial \mathscr{I}}{\partial \mathscr{U}} - 6\frac{\partial \mathscr{R}}{\partial \mathscr{V}} = 0 \end{aligned} \tag{35}$$

(Courant and Friedrichs, 1948).

Introducing the Riemann invariants $P = \frac{1}{2}(\mathscr{V} + \mathscr{U})$ and $\Sigma = \frac{1}{2}(\mathscr{V} - \mathscr{U})$, (35) can be rewritten

$$\begin{aligned} &\frac{\partial \mathscr{R}}{\partial \Sigma} = \frac{1}{6}(P - \Sigma + 1)\frac{\partial \mathscr{I}}{\partial \Sigma} , \\ &\frac{\partial \mathscr{R}}{\partial P} = \frac{1}{6}(P - \Sigma - 1)\frac{\partial \mathscr{I}}{\partial \Sigma} . \end{aligned} \tag{36}$$

In the $P - \Sigma$ plane, the characteristics are mapped into straight lines $P =$ const., $\Sigma =$ const.

Eqs. (36) are particularly easy to integrate as each equation is differentiated only with respect to one independent variable. The numerical integration was carried out by obtaining the image of the region LMON (Fig. 6) in the $P - \Sigma$ plane, and then integrating along the characteristics $P =$ const., $\Sigma =$ const. after having duly converted the boundary values (29), (30), (32) and (33).

The results of these integrations are shown in Figs. 7 to 12 for three different wind velocities, viz 0, 20 and 100 km/s. In the case of the zero wind velocity, the path of the front in the $\mathscr{R} - \mathscr{I}$ plane is

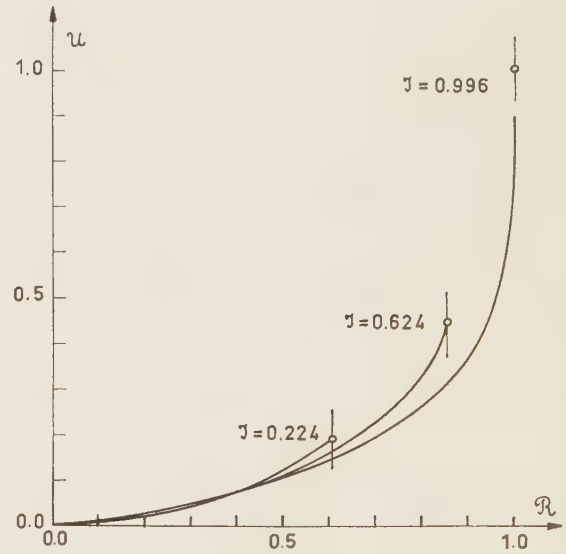

Fig. 7. The velocity $\mathscr{U}$ of the ionized gas at three different times as a function of the distance from the origin, the central star being at rest (spherical I-front). The vertical lines indicate the position of the I-front. $\mathscr{U}$ is measured in the units a_2 km/s

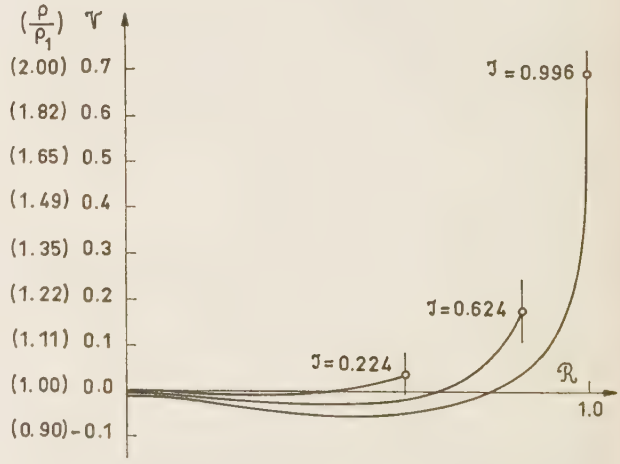

Fig. 8. The density of the ionized gas as a function of the distance from the origin. The ordinates show $\mathscr{V} = \ln(\varrho/\varrho_1)$, ϱ being the ionized gas density and ϱ_1 the neutral gas density. The values of (ϱ/ϱ_1) are shown in brackets

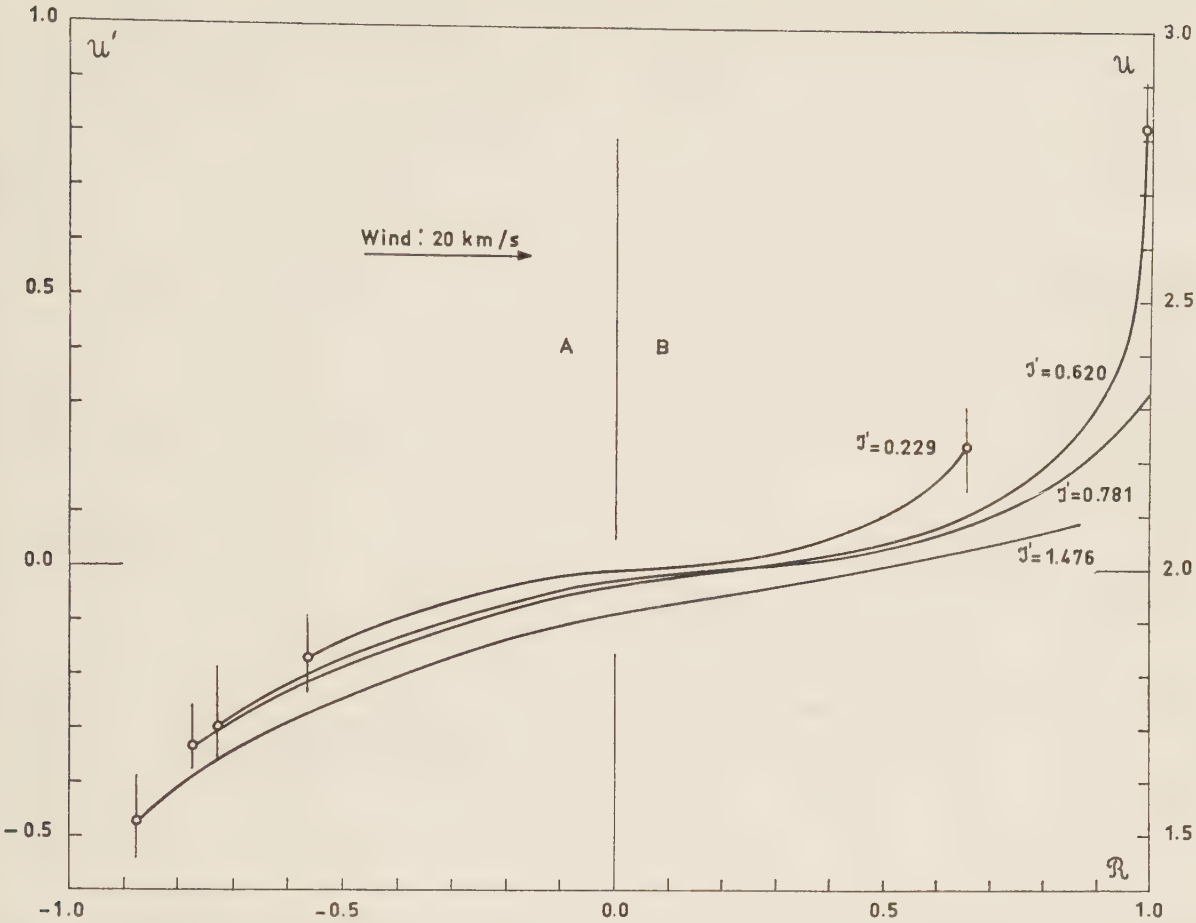

Fig. 9. The velocity of the ionized gas at 4 different times shown as a function of the distance $\mathscr{R}$, the central star moving at 20 km/s. The vertical lines indicate the position of the I front upstream (region A) and downstream (region B). The velocities (measured in terms of the sound velocity a_2) are shown in two different frameworks: $\mathscr{U}$, when the star is at rest and the neutral gas moves at 20 km/s, and $\mathscr{U}'$ when the star moves at 20 km/s and the neutral gas is at rest

given simply by $\mathscr{I} = \pm \mathscr{R}^3$ whereas the front velocity $\mathscr{V}_{FA}$ and $\mathscr{V}_{FB}$ in (24) and (25) is equal to $2/\mathscr{R}^2$. The results in this case are of course qualitatively identical with those obtained by Vandervoort (1963a, b).

In the figures, $\mathscr{U}$ and $\mathscr{V}$ have been plotted as functions of $\mathscr{R}$ for different values of $\mathscr{I}$. The brackets against $\mathscr{V}$ indicate the actual values of the density ratio ϱ_2/ϱ_1. One of the times chosen corresponds always to the appearance of a shock in region B, the other times being before or after. In the spherical case, the results are symmetrical for regions A and B, except that $\mathscr{U}$ and $\mathscr{V}$ change sign, and we have chosen only one of these regions.

In all the figures, the wind velocity is reduced by the front in region A, and the ionized gas is then continuously accelerated through both the regions until it reaches the front in region B. At the centre, the velocity is strictly zero at all times in the spherical case, whereas in the non-spherical case it is slightly less than the original velocity and decreases gradually with time. The density curves show that the gas is compressed behind the front in region A; the density then falls towards the centre to reach almost its original value, and increases again as the gas is compressed behind the front B. At any given point the density decreases with time after the passage of the front.

However, the most interesting feature is that the motion of the central star produces a marked asymmetry in the distribution of the density and the velocity around the star, this asymmetry becoming more and more pronounced with increasing time and wind velocities. In the following discussion it is more useful to speak in terms of a framework in which the neutral gas is at rest and the star itself

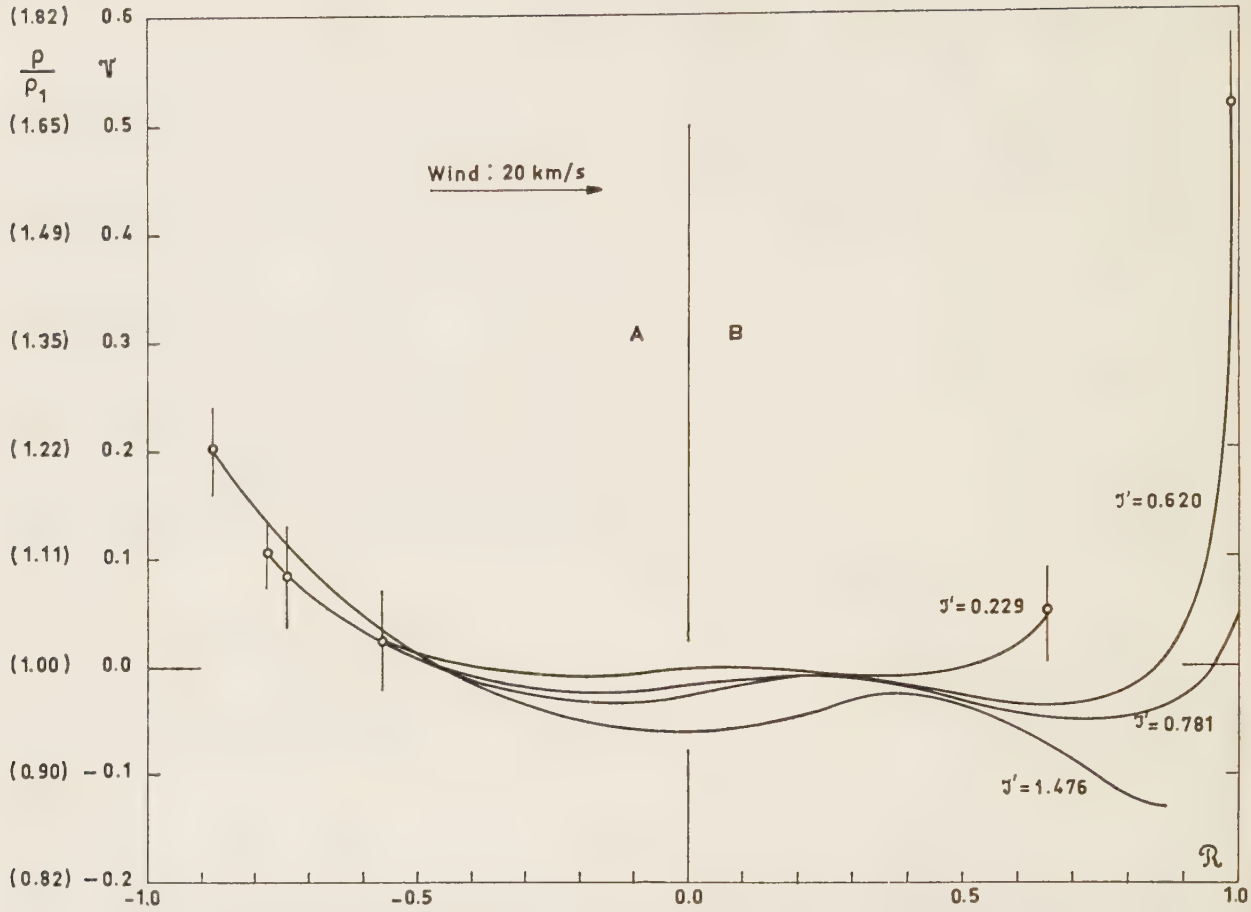

Fig. 10. The densities of the ionized gas for the case discussed in Fig. 9. The ordinates are as in Fig. 8

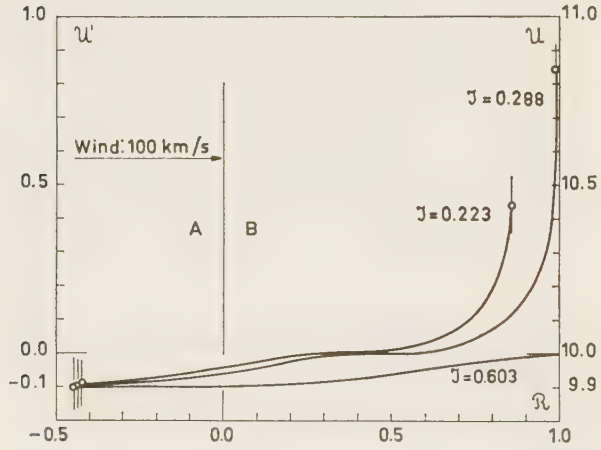

Fig. 11. Same as Fig. 9, but with the central star moving at 100 km/s

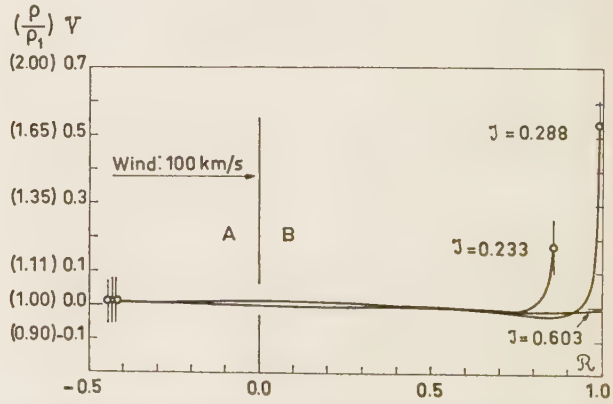

Fig. 12. Same as Fig. 10, but with the central star moving at 100 km/s

moves with the velocity $\mathscr{V}_*$. The $\mathscr{V}$ values remain unchanged in the density curves, whereas we have marked $\mathscr{U}' = \mathscr{U} - \mathscr{V}_*$ in the velocity curves.

The asymmetry in the curves is obviously due to the fact that the shock is formed much earlier in region B than in region A. Thus, when there is already a considerable velocity field and a strong compression in region B, at least near the I-front, both, the velocities and densities are closer to their original values in region A. Thus, for $V_* = 20$ km/s, a shock forms in region B at $\mathscr{I} = 0.64$. The ionized gas streams towards the front at a velocity of about 10 km/s and is compressed by a factor of two, whereas in region A, the gas velocity at the front is only 3 km/s, and the compression ratio is about 1.1.

This asymmetrical behaviour is shifted to ealier and earlier times as the velocity of the star increases, and is produced already at $\mathscr{I} = 0.3$ for $V_* = 100$ km/s, for instance. The I-front in front of the star has to travel at least with the stellar velocity, and if the latter is high, the I-front will remain continuously of the weak R-type. The gas velocities and density changes remain close to zero in most of the ionized region to rise very sharply near the I-front behind the star (region B). This behaviour is particularly evident in Figs. 11 and 12, the density changes being even more rapid than the velocity changes.

To conclude, the asymmetric behaviour and rapid density and velocity changes only on one side of the star for sufficiently high stellar velocities make the dynamics of non-spherical H II regions worth investigating in greater detail. In the next publication the author hopes to treat the problems of regions with shocks.

Acknowledgements. It is a pleasure to thank Profs. E. Schatzman and J. P. Guiraud for many useful talks and discussions.

References

Axford, W. I. 1961, Phil. Trans. R. Soc. London, A **253**, 301.
Axford, W. I. 1964a, Ap. J. **139**, 761.
Axford, W. I. 1964b, Ap. J. **140**, 112.
Byrd, P. F., and Friedman, M. D. 1954, Handbook of Elliptic Integrals for Engineers and Physicists, Springer-Verlag, Berlin-Göttingen-Heidelberg.
Courant, R., and Friedrichs, K. O. 1948, Supersonic Flow and Shock Waves, Chs. II and III, Interscience Publishers, New York, London.
Courant, R., and Hilbert, D. 1962, Methods of Mathematical Physics, Vol. II, Interscience Publishers, New York, London.
Goldsworthy, F. A. 1961, Phil. Trans. R. Soc. London, A **253**, 277.
Gould, R. J. 1963, Ph. D. Thesis, Cornell University.
Gröbner, W., and Hofreiter, N. 1949, Integraltafel, Erster Teil, Springer-Verlag, Wien und Innsbruck.
Kahn, F. D. 1954, B. A. N., **12**, 187.
Kaplan, S. A. 1957, Astr. Zh. **34**, 183.
Landau, L. D., and Lifschitz, E. M. 1959, Fluid Mechanics Pergamon Press, London, New York.
Lasker, B. M. 1966, Ap. J. **143**, 700.
Mathews, W. G. 1965, Ap. J. **142**, 1120.
Savedoff, M. P., and Greene, J. 1955, Ap. J. **122**, 477.
Vandervoort, P. O. 1963a, Ap. J. **137**, 381.
Vandervoort, P. O. 1963b, Ap. J. **138**, 426.
Vandervoort, P. O. 1964, Ap. J. **139**, 869.
Vandervoort, P. O. 1966, Ap. J. **146**, 104.

M. Rasiwala
Institut d'Astrophysique
98 bis Bld Arago Paris 14, France

Printed in Germany by Brühlsche Universitätsdruckerei Giessen